GEOSCIENCE FRONTIERS 3(1) (2012) 59–71

available at www.sciencedirect.com

China University of Geosciences (Beijing)

GEOSCIENCE FRONTIERS

journal homepage: www.elsevier.com/locate/gsf

ORIGINAL ARTICLE

Tourmalinization at the Darasun goldfield, Eastern Transbaikalia: Compositional, fluid inclusion and isotopic constraints

Vsevolod Prokofiev [a,b,*], Ivan Baksheev [b], Lidiya Zorina [c], Boris Belyatsky [d], Vladimir Ustinov [e], Nadezhda Krivitskaya [b]

[a] *Institute of Geology of Ore Deposits, Petrography, Mineralogy & Geochemistry, Russian Academy of Sciences, Moscow, Russia*
[b] *Lomonosov Moscow State University, Moscow, Russia*
[c] *Vinogradov Institute of Geochemistry, Irkutsk, Russia*
[d] *Institute of Precambrian Geology and Geochronology, RAS, Saint-Petersburg, Russia*
[e] *Vernadsky Institute of Geochemistry and Analytical Chemistry, RAS, Moscow, Russia*

Received 21 March 2011; accepted 21 July 2011
Available online 9 September 2011

KEYWORDS
Tourmaline composition;
Fluid inclusions;
Oxygen isotopes;
Gold deposits;
Transbaikalia;
Russia

Abstract Zoned tourmaline (schorl-dravite) in the matrix of hydrothermal explosive breccia and ore veins in gold deposits, Chita region, Eastern Transbaikalia, Russia, are associated with Na- and K-rich porphyry-type subvolcanic intrusives. $\delta^{18}O$ values of tourmaline from three gold deposits (Darasun, Talatui, Teremkinskoye) are +8.3‰, +7.6‰, and +6.0‰ and calculated $\delta^{18}O$ values of fluids responsible for the tourmalinization are +7.3‰, +7.7‰, and +4.2‰, respectively. These data imply an igneous fluid source, except at the Teremkin deposit where mixing with meteoric water is indicated. Wide ranges of Fe^{3+}/Fe_{tot} and the presence of vacancies characterize the Darasun deposit tourmaline indicating wide ranges of $f(O_2)$ and pH of mineralizing fluids. Initial stage tourmalines from the gold deposits of the Darasun ore district are dravite or high mg schorl. Second stage tourmaline is characterized by oscillatory zoning but with Fe generally increasing towards crystal rims indicating decreasing temperature. Third

* Corresponding author. Lomonosov Moscow State University, Moscow, Russia.
E-mail address: vpr@igem.ru (V. Prokofiev).

Peer-review under responsibility of China University of Geosciences (Beijing).
doi:10.1016/j.gsf.2011.07.006

stage tourmaline formed unzoned crystals with x_{Mg} (mole fraction of Mg) close to that of the first stage tourmaline, due to a close association with pyrite and arsenopyrite. From Fe^{3+}/Fe_{tot} values, chemical composition and crystallization temperatures, $\log f(O_2)$ of mineralizing fluids ranged from ca. −25 to −20, much higher than for the gold-bearing beresite–listvenite association, indicating that tourmalinization was not related to gold mineralization.

1. Introduction

Gold deposits in the Eastern Transbaikalia area of Russia are widespread along the Mongolian–Okhotsk suture zone (Zorin et al., 1998). The formation of these deposits is considered to be related to the end of collision between the Mongolian and Siberian continents and subsequent rifting (Zorin et al., 1998, 2001). Deposits in the Darasun gold-bearing area are one of the main types of gold mineralization in Eastern Transbaikalia, and locally referred to as the "Darasun type" (Timofeyevsky, 1972). The deposits are also referred to the gold-porphyry or gold-copper-porphyry-type (Prokof'yev et al., 2000; Sillitoe, 2000), and there are many studies of the gold deposits (Timofeyevsky, 1972; Prokof'yev et al., 2000; Prokof'ev et al., 2000; Sakharova, 1972; Lyakhov, 1975; Zorina, 1993; Prokof'ev and Zorina, 1994; Yurgenson and Yurgenson, 1995; Prokof'ev et al., 2004, 2005a,b). After a long duration of no or minimal mining, the gold deposits of the Darasun area deposits are again mined and reinvestigated. Tourmaline along with quartz is one of the most widespread gangue mineral of the gold deposits (Fig. 1). This mineral shows a wide range of chemical composition and can be used as an indicator of the geological environment of gold mineralization (e.g., Slack, 1996). In this paper, an electron microprobe, Mössbauer spectroscopy, oxygen isotope, and Sm–Nd dating study of tourmaline and of fluid inclusions in coeval quartz were carried out to determine the *p-T*-fluid environment of tourmalinization.

2. Geological setting

The Darasun gold mine is located in the Chita region of Eastern Transbaikalia (Fig. 2) and for a long time was the second most productive gold mine in the area. In 2004, mining of this deposit was resumed. In addition, the Talatuy medium-sized and the Teremki small-sized gold deposits are also mined in the Darasun district (Fig. 2). All three deposits are mainly hosted in basic igneous rocks. The oldest rock is an Early Paleozoic metagabbro that is intruded by Middle Paleozoic and Middle Mesozoic granodiorite, diorite, granite, granosyenite, syenite, and by Early Jurassic granitoids of the Amanan Complex. It is generally considered that the formation of gold deposits in Eastern Transbaikalia is related to small subvolcanic alkali-rich intermediate and felsic intrusions (Timofeyevsky, 1972; Prokof'ev and Zorina, 1996). These igneous rocks form part of the Amudzhikan–Sretensky Complex of Middle to Late Jurassic age (?) and are represented by plagiogranite- and granodiorite-porphyry fracture-type intrusions and stocks (Fig. 3a), quartz-diorite porphyry, granophyre, felsite, and pitchstone dykes. However, the ore vein/subvolcanic rock volume ratio indicates that the felsic magmas cannot have provided the necessary amount of ore elements, including Au, Ag, Bi, and Te, for the gold mineralization, and that a larger, deeper source is required for the formation of the minor intrusions and mineralization.

The Darasun deposit comprises more than 200 steeply-dipping gold-bearing quartz veins, and mineralized zones associated with subvolcanic K-rich granodiorite-porphyry. Pipe-like bodies of hydrothermal explosive breccia cemented with quartz, tourmaline and sulfide minerals occur in the endocontact zone of this body and are considered to be feeders (Prokof'ev et al., 2000). Ores are enriched in sulphides (40%–60%) and Bi- and Te-bearing minerals. Pyrite, arsenopyrite, chalcopyrite, pyrrhotite, fahlore, sphalerite, galena, Cu, Ag, As, Bi, Pb sulfosalts, tellurides and native gold are the major ore minerals. A large amount of arsenopyrite in veins is a special feature of the Darasun deposit, and is related to a high a_{As} in the mineralizing fluid, which also resulted in the precipitation of native arsenic Quartz, tourmaline (Fig. 3c), calcite, gypsum, and anhydrite are gangue minerals.

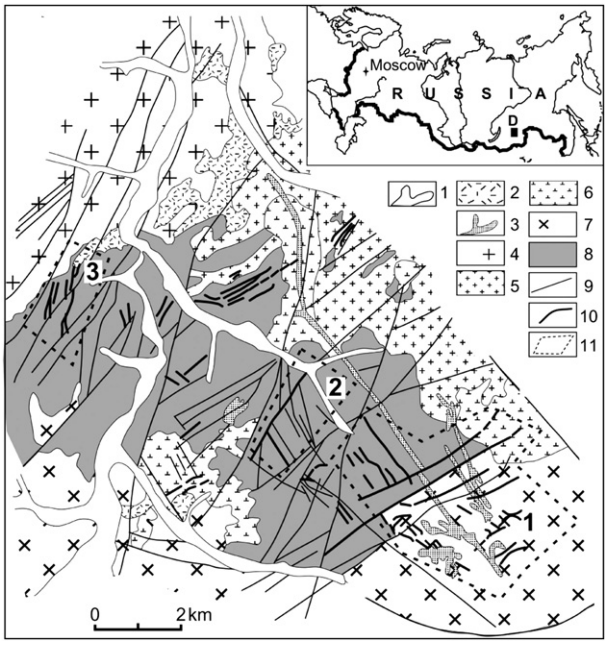

Figure 1 Location of the Darasun goldfield (D) and geological sketch map (adopted from the Darasun exploration expedition). 1: alluvium; 2–3: Middle-Upper Jurassic Amudzhikan–Sretensky complex, 2: volcanics, 3: porphyry sub-volcanics and dykes: diorite porphyry, granodiorite-porphyry, granite-porphyry and others; 4: biotite-hornblende granite and granodiorite of the Triassic Amanansky complex; 5–6: Upper Paleozoic – Lower Mesozoic Olyokminsky complex, 5: biotite and leucogranite, 6: syenite, granosyenite, quartz syenite; 7: diorite, quartz diorite, granodiorite of the Middle Paleozoic Krestovsky complex; 8: metamorphosed gabbroids (gabbro, amphibolite, gabbro-diorite, troctolite) of the Lower Paleozoic Kruchininsky complex; 9: faults; 10: ore bodies; 11: deposits, 1: Darasun, 2: Teremki, 3: Talatuy.

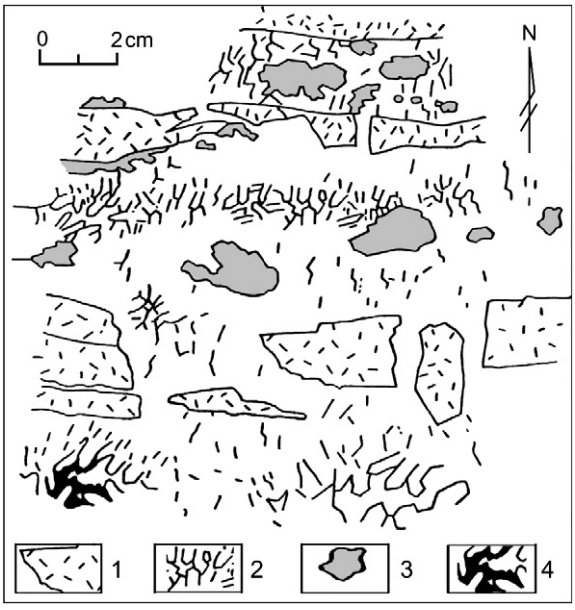

Figure 2 Section of gold ore vein Glavnaya of the Darasun deposit (modified after Timofeyevsky, 1972). 1: quartz–tourmaline aggregate; 2: euhedral quartz crystals; 3: pyrite; 4: sulfosalts in miarole.

The Teremki deposit is located 5 km north-west of the Darasun deposit and comprises closely spaced gently to steeply-dipping gold-bearing sulfide-tourmaline-quartz veins and mineralized zones. The veins and zones occur beneath Amudzhikan Complex felsic rocks. Ore mineralization is similar to that of the Darasun deposit, but the sulfide content is less than 20%. The tourmaline content is higher than at Darasun. Pyrite, arsenopyrite, chalcopyrite, galena, sphalerite, Ag, Bi, Pb sulfosalts, and native gold are the major ore minerals. Quartz, tourmaline (Fig. 3d), and carbonates are gangue minerals.

The Talatuy deposit is located 12 km north-west of the Darasun deposit, and is characterized by complex mineralized zones associated with dikes of diorite porphyry, lamprophyre, granodiorite-porphyry, quartz-porphyry, and granite-porphyry of Middle to Late Jurassic age (?). Ore minerals occur in veinlets and impregnation zones. Pyrite, chalcopyrite, magnetite, hematite, ilmenite, native gold, scheelite, and pyrrhotite (mainly intergrown in pyrite and chalcopyrite) are the major ore minerals. Minor martitization and mushketovitization are present, indicating fluctuation of $f(O_2)$ during mineralization. Tourmaline (Fig. 3b), epidote, titanite, chlorite, quartz, carbonates, biotite, orthoclase, and chalcedony are gangue minerals.

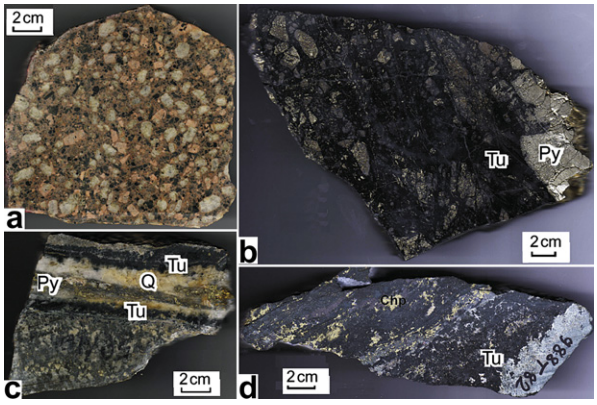

Figure 3 Host rock and ores of the Darasun goldfield. a: granodiorite-porphyry of Amudzhikan–Sretensky complex; b: pyrite–quartz–tourmaline gold ore of Talatuy deposit; c: gold ore vein of Darasun deposit; d: chalcopyrite–quartz–tourmaline gold ore vein of Teremki deposit. Tu – tourmaline (black); Q – quartz; Py – pyrite; Chp – chalcopyrite. Scale bar is 2 cm.

3. Occurrences of tourmaline

Tourmaline in the Darasun ore veins occurs as brown and light to dark-green needles up to 150 μm long or as radiating fibrous aggregates. At least two generations of tourmaline can be distinguished; first generation tourmaline (tourmaline I) which forms sectorial and concentrically zoned crystals; second generation tourmaline (tourmaline II) which occurs as divided crystals, devoid of internal zoning, that overgrow tourmaline I (Fig. 4). Both generations of tourmaline exhibit different pleochroism, color and intensity that are determined by the different amounts of Fe^{2+} and Fe^{3+} present.

Tourmaline from the Teremki deposit occurs as black, isolated crystals up to 200 μm long or crystal aggregates. The tourmaline is unzoned and strongly pleochroic from light-yellow to dark-green.

Tourmaline in the Talatuy deposit forms isolated dark-green crystals up to 200 μm long or crystal aggregates. The tourmaline is zoned and has light to dark-green pleochroism. It is associated with magnetite, early pyrite and chalcopyrite, and is replaced by sulfides of the ore-forming stage.

4. Analytical techniques

The chemical composition of tourmaline has been determined by a CAMEBAX SX-50, electron probe microanalyser (I.A. Bryzgalov analyst) at the Division of Mineralogy, Lomonosov Moscow State University, and a CAMECA SX-100 instrument (N.N. Kononkova, analyst), at the Vernadsky Institute of Geochemistry and Analytical Chemistry, RAS, Moscow. An accelerating potential of 15 kV, and sample current intensity 30 nA

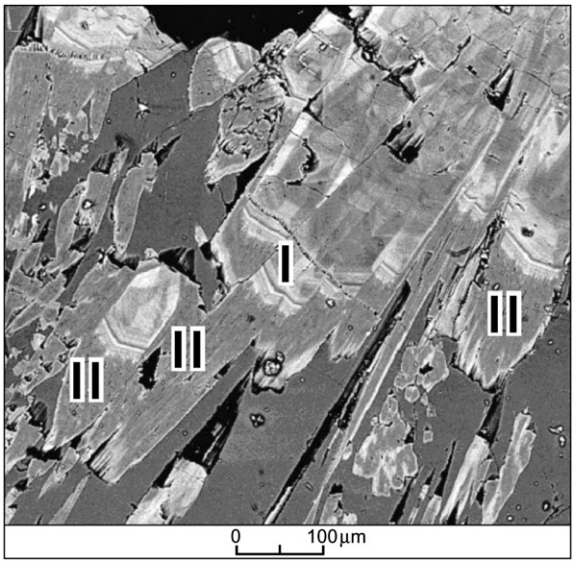

Figure 4 BSE image of the divided tourmaline II crystals overgrowing optically and chemically zoned tourmaline I crystals. Dotted line = iron content along profile (Fig. 3).

were used with a beam diameter ~3 μm. PAP corrections were used for element correction procedures. The following standards were used: hornblende (Si, Al, Ca, Mg, Fe), orthoclase (K), albite (Na), fluorphlogopite (F), pyrophanite (Mn, Ti), vanadinite (V), NiO (Ni), Cr_2O_3 (Cr).

A Mössbauer study was carried out at the Institute of Mineralogy, Urals Branch of RAS, Miass, Russia. ^{57}Fe spectra were recorded using a conventional Mössbauer spectrometer operating in constant acceleration mode with a ^{57}Co (in Cr) source at room temperature (A.B. Mironov, analyst). Isomer shift is referred to an α-Fe absorber at 293 K. These spectra were analyzed using standard computer techniques.

Fluid inclusions have been studied using double polished thin sections (typical size: 25 mm × 25 mm × 0.5 mm), first optically, then with a THMSG-600 'Linkam' freezing/heating stage equipped with an Olympus-80 objective at IGEM, RAS, Moscow. Precision at low temperature (cooling) was about 0.7 °C and about 2 °C at high temperatures (heating). Salinity was estimated from the final ice melting temperature (T_m). Pressure was determined using syngenetic gas-dominated and aqueous saline inclusions trapped during fluid boiling.

Bulk inclusion analysis by gas chromatography, ion chromatography, and ICP-MS has been carried out in the TsNIGRI, Moscow. The first technique used a 'Tzevet-100M' chromatograph (Y.V. Vasyuta, analyst). The second technique used a 'Tzvet 3006' chromatograph (Y.V. Vasyuta, analyst). The detection limit of these techniques was 0.001 μg L^{-1}; ICP-MS used a 0.0004–0.3 μg L^{-1}.

Oxygen isotopes were determined at GEOKHI RAS, Moscow. A fluoride procedure was applied to extract oxygen from tourmaline. Extracted oxygen was analyzed for isotopic composition ($\delta^{18}O$ relative to SMOW) by mass spectrometer with a reproducibility of ±0.2‰ (Ustinov, 1983). The $\delta^{18}O$ value of fluids responsible for tourmalinization was calculated from the equation of Zheng (1993) taking into consideration fluid inclusion temperatures.

Sr and Nd isotope composition as well as Rb, Sr, Sm, Nd contents in minerals were determined by isotope dilution using a solid phase multi-collector mass-spectrometer TRITON (CIR VSEGEI) at St. Petersburg. The elements were extracted according to the conventional method of chromatographic separation (Richard et al., 1976). Measurement errors for isotope ratios $^{147}Sm/^{144}Nd$, $^{87}Rb/^{86}Sr$ were about 0.3%, for Rb, Sr, Sm, Nd content −0.5%. Measurement error for isotope composition of Sr, Nd was <0.005%. Reproducibility of analytical data was checked by measuring international standards such as La-Jolla, BCR-1, 2, SRM-987 and corresponds to ±0.005%.

5. Results

5.1. Chemical composition of tourmaline

The composition of tourmaline from the different gold deposits is similar. However, tourmalines from each deposit show some individual features.

Tourmaline I from the Darasun deposit shows oscillatory zoning elongated parallel to the c-axis related to variation of iron content (Fig. 5). Central areas of crystals are dravite and "oxy-dravite" enriched in Fe with ($Fe_{tot}/(Fe_{tot} + Mg)$ = 0.33–0.35, Ca/(Ca + Na) = 0.10–0.30, and ^{W}OH (relations $Fe_{tot}/(Fe_{tot} + Mg)$ and Ca/(Ca + Na) characterize composition of the tourmaline) = 0.201–0.900). Marginal parts of the zoned crystals have compositions of Fe-rich dravite to "oxy-dravite" with (Fe/(Fe + Mg) = 0.35–0.48, Ca/(Ca + Na) = 0.08–0.35, and ^{W}OH = 0.006–0.810). Dravite to "oxy-dravite" tourmaline compositions from explosion breccia with ($Fe_{tot}/(Fe_{tot} + Mg)$ = 0.05–0.11, Ca/(Ca + Na) = 0.02–0.11, and ^{W}OH = 0.390–0.800), and schorl to "oxy-schorl" compositions with ($Fe_{tot}/(Fe_{tot} + Mg)$ = 0.61–0.74, Ca/(Ca + Na) = 0.04–0.29, and ^{W}OH = 0–0.640) in the deep levels of this deposit are also regards as examples of tourmaline I. These tourmalines exhibit the highest vacancy content up to 0.335 apfu (atoms per formula unit) and 0.458 apfu, respectively. Tourmaline with very high Fe^{3+} (up to 4.076 apfu) was detected in one sample and may indicate the presence of buergerite and povondraite components. Tourmaline II dravite and "oxy-dravite" compositions form intergrowths with early arsenopyrite and chalcopyrite. Compositionally, tourmaline II is an intermediate member of the dravite-"oxy-dravite" series with ($Fe_{tot}/(Fe_{tot} + Mg)$= 0.29–0.33, Ca/(Ca + Na) = 0.20–0.23, and ^{W}OH = 0.290–0.550). Most vein tourmaline with compositions of ($Fe_{tot}/(Fe_{tot} + Mg)$ = 0.09–0.49, Ca/(Ca + Na) = 0.09–0.40, ^{W}OH = 0.072–0.814) is also considered to represent tourmaline II. Both generations of tourmaline contain small amounts of Cu (up to 0.020 apfu), Zn (up to 0.025 apfu), and F (up to 0.37 apfu).

In the ternary $Fe_{70}Al_{30}$-Al-$Mg_{70}Al_{30}$ plot (Fig. 6a), tourmaline compositions from Darasun show a trend from relatively Fe-poor to Fe-rich varieties. Most compositions plot below the schorl-dravite join.

The two generations of tourmaline are not clearly recognized in the Talatuy deposit. Nevertheless, like at Darasun, there are two crystal types with different compositional zoning. Tourmaline associated with magnetite and show only a small increase in $Fe_{tot}/(Fe_{tot} + Mg)$ from core to rim (0.45 → 0.56, 0.56 → 0.64).

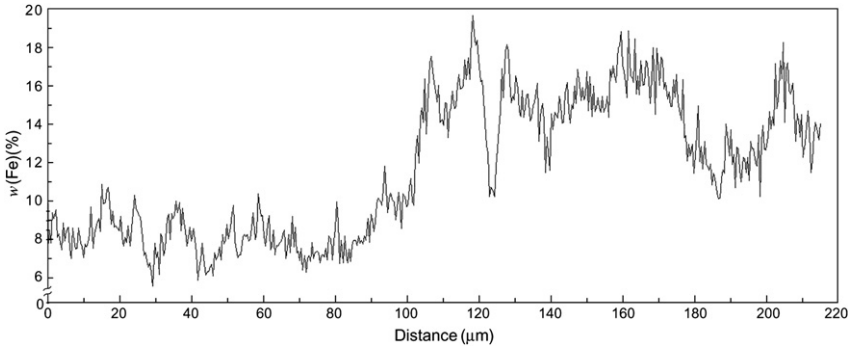

Figure 5 Oscillatory zoning of iron content along profile through single tourmaline crystal shown in Fig. 2.

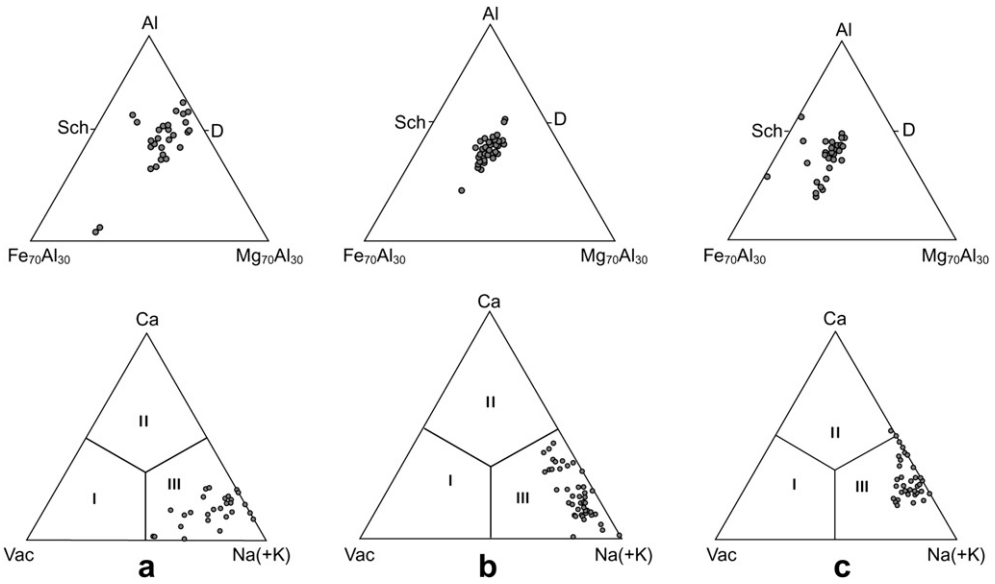

Figure 6 Fe–Al–Mg and Vac (vacancy)–Ca–Na(+K) plots for tourmalines from the Darasun goldfield deposits. a: Darasun; b: Talatuy; c: Teremki. I: vacancy group; II: calcic group; III: alkali group. Sch: schorl; D: dravite.

Tourmaline associated with early pyrite and chalcopyrite has a similar compositional zonation to tourmaline II at Darasun. In these oscillatory zoned crystals, the $Fe_{tot}/(Fe_{tot} + Mg)$ ratio shows an overall decrease from core to rim (0.53 → 0.50 → 0.48 → 0.44; 0.45 → 0.55 → 0.39). In general, $Fe_{tot}/(Fe_{tot} + Mg)$ ranges from 0.36 to 0.64. ^{W}OH and Ca/(Ca + Na) range from 0.000 to 0.985 apfu and from 0.01 to 0.45, respectively. Therefore, tourmaline from the Talatuy deposit can be classed as an intermediate member of the dravite ("oxy-dravite") – schorl ("oxy-schorl") series. Zinc (up to 0.010 apfu) is slightly less than in tourmaline from the other gold deposits, and Cu is slightly higher (up to 0.037 apfu). Maximum fluorine content is 0.230 apfu and similar to F values in the Darasun tourmaline.

In the ternary $Fe_{70}Al_{30}$-Al-$Mg_{70}Al_{30}$ plot (Fig. 6b), tourmaline compositions from Talatuy show a trend from relatively Fe-poor to Fe-rich varieties. Most compositions plot below the schorl-dravite join.

Only one type of tourmaline composition is present in the Teremki deposit (Fig. 6c). This tourmaline is associated with early sulfides and the composition is similar to tourmaline II from Darasun and the later tourmaline from Talatuy. The tourmaline has Fe-rich cores ("oxy-schorl") with ($Fe_{tot}/(Fe_{tot} + Mg) = 0.74–0.98$, $Ca/(Na + Ca) = 0.20–0.31$, and $^{W}OH = 0–0.48$ apfu), and Mg-richer rims that crystallized with sulfides. The rim compositions represent an intermediate member of the dravite ("oxy-dravite")–schorl ("oxy-schorl")–feruvite series with ($Fe_{tot}/(Fe_{tot} + Mg) = 0.49–0.64$, $Ca/(Na + Ca) = 0.20–0.53$, $^{W}OH = 0.150–0.923$ apfu). Zn (up to 0.026 apfu) in the Teremki tourmaline is the same as the Darasun tourmaline; Cu and F are less and up to 0.009 apfu and 0.088 apfu, respectively.

In the ternary $Fe_{70}Al_{30}$-Al-$Mg_{70}Al_{30}$ plot (Fig. 6c), the Teremki tourmalines trend from relatively Fe-poor to Fe-rich varieties and, most compositions plot are below the schorl-dravite join, although some compositions correspond to Mg-free tourmaline.

On the basis of Mössbauer spectra (Prokof'ev et al., 2005a, b), the Fe^{3+}/Fe_{tot} of the tourmaline from Darasun is 0.47–0.85, from Talatuy ~ 0.67, and from Teremki ~ 0.51.

5.2. Fluid inclusions

Primary, pseudosecondary, and secondary fluid inclusions were recognized in quartz from breccia matrix and ore veins of all gold deposits. On the basis of phase composition at room temperature, these inclusion can be divided into three types: B – three- and multiphase inclusions of chloride brine, A – two-phase inclusions of aqueous solution, and G – gas-dominated inclusions, containing water vapor with liquid water meniscus and sometimes liquid CO_2 (Fig. 7). Type G fluid inclusions are generally syngenetic with B and A types. This indicates fluid immiscibility during tourmalinization.

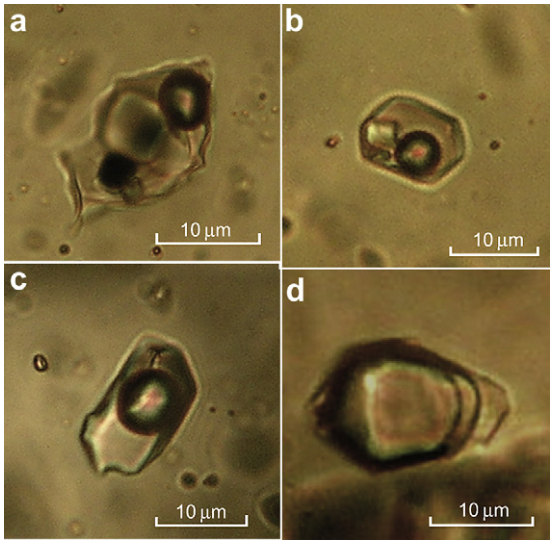

Figure 7 Types of fluid inclusions in quartz from quartz–tourmaline assemblage in the Darasun goldfield deposits (all photographs were taken at room temperature): a, b: multiphase inclusions of chloride brine (B); c: two-phase inclusion of aqueous solution (A); d: gas-dominated inclusion with the CO_2 rim (G). Length of the bar is 10 μm.

Table 1 Summary of fluid inclusion data.

Mineral	Inclusion type	*n**	T_h (°C)	Homogeneous mode	T_m CO_2 (°C)	T_h CO_2 (°C)	Homogeneous mode CO_2	T_m Clathrate (°C)	Eq. *w*(NaCl) (%)	ρ (g/cm^3)	*p* (bar)
						Darasun					
						Explosive breccia					
Qz	B	117	618–230	Liquid					50.3–28.8	1.11–0.78	1460–300
	A	47	543–170	Liquid					26.4–3.2	1.00–0.65	
	G	19	557–269	Vapor	−59.3	23.3	Vapor	8.2	28.9–3.2	0.51–0.22	890–260
						Early stage					
Qz	B	32	412–230	Liquid					44.8–29.3	1.08–0.89	2040–65
Qz	A	376	399–280	Liquid					24.1–1.4	1.04–0.88	
Qz	G	155	429–290	Vapor	−56.6 to −59.0	24.7 to −40.0	Liquid to vapor	9.1–5.1	21.3–0.7	0.77–0.20	1560–110
						Main stage					
Sph	A	117	383–160	Liquid					16.8–0.7	0.98–0.70	
Qz	A	207	340–210	Liquid					22.0–2.2	0.97–0.66	
Anh	A	18	247–214	Liquid					15.5–14.8	0.97–0.94	
						Late stage					
Qz	A	52	223–124	Liquid					17.0–2.2	1.04–0.90	
Calc	A	5	209	Liquid					10.9	0.94	–
						Teremki					
						Early stage					
Qz	B	23	466–295	Liquid					41.0–28.0	1.10–0.88	
Qz	A	507	438–300	Liquid					26.3–4.0	0.99–0.47	
Qz	G	333	443–320	Vapor	−56.8 to −58.2	11.5 to −53.0	Vapor	8.6–8.0	8.1–1.2	0.48–0.02	410–80
						Main stage					
Qz	A	120	298–216	Liquid					26.3–4.2	0.99–0.82	
						Late stage					
Qz	A	61	195–118	Liquid					27.8–2.6	1.10–0.89	
						Talatuy					
						Early stage					
Qz	B	41	611–402	Liquid					56.3–29.9	1.25–0.78	2310–150
Qz	A	6	495–469	Liquid					23.2–0.7	0.54–0.49	
Qz	G	17	589–431	Vapor	−56.7 to −58.9	31.0 to −49.3	Vapor	–	17.6–0.9	0.57–0.02	1040–360
						Main stage					
Qz	B	97	397–269	Liquid					48.4–29.3	1.21–0.97	
Qz	A	105	438–273	Liquid					24.1–1.4	0.91–0.47	
Qz	G	40	377–292	Vapor	−56.6 to −59.0	24.7 to −40.0	Vapor	8.6–7.9	8.0–1.4	0.42–0.03	730–150
						Late stage					
Qz	A	18	251–133	Liquid					5.4–0.4	1.03–0.88	
Calc	A	19	231–146	Liquid					2.1–0.7	0.94–0.83	–

Notes: * – number of inclusions. Inclusion type: B – three- and multiphase inclusions of chloride brine, A – two-phase inclusions of aqueous solution, and G – gas-dominated inclusions, containing water vapor with liquid water meniscus and sometimes liquid CO_2. Qz – quartz, Calc – calcite, Sph – sphalerite, Anh – anhydrite.

Table 2 Chemical composition of mineralizing fluids in the Darasun goldfield deposits (16 samples of quartz).

Component	Darasun						Talatuy			Teremki						
	1*	2*	3*	4*	5*	6*	7*	8*	9*	10*	11*	12*	13*	14*	15*	16*
	Breccia			Veins			Ores			Veins						
CO_2 (g/kg) of water	10.02	20.96	2.40	142.86	147.32	98.34	10.47	49.75	16.20	15.04	35.19	11.87	35.93	20.80	6.54	29.33
CH_4 (g/kg) of water	1.75	0.12	0.27	2.40	4.87	1.57	0.08	0.33	0.35	0.30	0.12	0.07	0.72	0.05	0.07	3.46
Cl^- (g/kg) of water	22.68	9.64	23.19	15.43	17.90	13.43	108.33	71.83	84.74	8.03	21.60	3.78	21.85	4.27	7.27	2.49
HCO_3^- (g/kg) of water	69.16	110.35	619.87	368.58	473.10	135.56	50.00	56.643	83.50	287.36	41.20	52.97	77.75	20.82	2.52	205.31
Na (g/kg) of water	27.49	10.09	10.57	66.65	75.04	14.64	52.03	36.715	54.51	10.94	13.25	6.98	28.86	5.11	4.50	7.68
K (g/kg) of water	41.82	2.11	4.78	71.57	122.71	33.90	20.45	24.77	27.71	5.15	3.90	2.24	2.76	1.11	0.92	15.32
Ca (g/kg) of water	4.37	30.49	159.55	23.28	21.08	11.46	18.13	11.50	11.05	72.57	8.37	9.32	11.79	3.71	0.48	37.75
Mg (g/kg) of water	1.75	0.92	31.22	6.86	8.87	6.28	2.66	2.25	0.94	8.64	2.46	4.32	2.76	0.29	0.08	9.63
Br (g/kg) of water	–	0.03	–	0.65	0.67	–	0.48	0.037	0.19	0.48	0.28	0.24	–	0.01	–	1.92
As (g/kg) of water	0.29	0.24	0.40	3.55	1.63	1.38	0.38	0.15	0.24	0.12	0.20	0.07	0.51	0.17	0.02	0.80
B (g/kg) of water	0.35	1.89	0.12	0.55	0.97	1.11	1.48	0.16	0.11	5.11	1.10	0.88	0.39	0.26	0.08	0.70
Sr (g/kg) of water	0.19	0.07	1.73	0.44	0.34	0.80	1.39	0.38	0.25	0.40	0.10	0.13	0.12	0.03	0.01	0.75
Ba (g/kg) of water	0.77	0.01	0.02	0.38	0.59	–	1.31	0.19	0.14	0.03	0.42	0.03	0.03	0.01	0.002	0.39
Cu (g/kg) of water	0.22	0.02	0.01	6.48	4.75	0.81	0.17	0.18	0.18	0.03	0.05	0.13	0.08	0.03	0.02	1.51
Zn (g/kg) of water	0.64	0.04	–	1.84	4.89	2.82	2.28	0.95	0.93	0.08	0.46	0.17	–	0.04	0.06	3.57
Mn (g/kg) of water	0.70	0.06	–	0.52	0.94	0.24	4.44	1.89	1.86	0.29	0.50	0.29	0.44	0.05	0.01	1.44
Fe (g/kg) of water	–	0.28	0.67	5.95	7.94	6.26	0.79	1.05	0.81	0.36	0.13	0.53	–	0.12	0.04	7.24
Rb (mg/kg) of water	148	4.46	23.80	98.30	118.50	90.50	120	67.30	91.80	10.10	15.80	5.85	21.6	2.44	1.84	32.90
Li (mg/kg) of water	17.80	22.90	17.20	149.50	176.60	214	62.80	24.20	43.90	79.30	2.78	84.2	6.12	29.00	16.40	90.70
Cs (mg/kg) of water	5.23	7.41	5.20	8.60	15.50	8.67	14.40	15.40	29.30	1.26	11.60	1.98	30.4	3.84	3.01	20.40
Mo (mg/kg) of water	68.50	42.16	11.20	1.00	–	51.50	0.70	2.59	11.50	27.50	2.74	64.3	4.22	3.15	4.37	17.20
Ag (mg/kg) of water	–	–	4.32	3.99	7.96	3.54	2.62	–	0.28	49.10	11.9	28.9	–	0.17	2.56	6.53
Sb (mg/kg) of water	18.30	4.01	79.70	1624	7506	319	4.90	6.94	5.66	15.30	1.90	6.62	15.3	36.60	0.61	208
Cd (mg/kg) of water	5.33	0.94	–	21.98	5.97	10.99	7.72	7.81	5.25	29.70	0.95	0.60	1.20	11.00	0.81	27.70
Pb (mg/kg) of water	67.1	3.38	–	129	165	49.80	62.40	7.41	22.60	5.50	25.2	121	16.8	3.92	0.68	96.20
Bi (mg/kg) of water	0.53	0.06	–	6.17	8.15	1.59	0.07	0.07	0.28	0.27	3.16	10.5	7.43	0.34	0.03	16.20
Co (mg/kg) of water	–	0.71	0.50	1.67	3.38	3.54	2.09	1.12	3.60	0.70	0.47	0.74	0.42	0.17	0.47	12.30
Ni (mg/kg) of water	–	23.20	6.07	31.40	34.20	43.70	17.30	9.81	12.40	17.00	11.80	11.9	3.61	3.68	6.12	267
Te (mg/kg) of water	–	5.72	2.49	–	–	–	–	–	–	–	0.29	0.45	–	1.70	0.77	–
Au (mg/kg) of water	–	–	0.37	0.90	0.80	1.71	–	0.42	–	–	0.06	3.00	–	0.02	0.008	1.39
Hg (mg/kg) of water	1.40	0.35	0.68	–	–	–	0.32	0.47	–	0.21	0.69	0.59	–	0.03	0.28	–
Tl (mg/kg) of water	0.72	0.39	1.00	1.90	0.60	1.22	3.30	1.70	3.30	0.91	1.05	0.99	0.46	0.20	0.21	–
ΣREE (mg/kg) of water	–	0.45	1.82	26.70	23.30	94.60	0.71	0.30	1.90	0.67	0.53	1.18	–	0.37	0.12	22.6
Na/K	0.70	4.80	2.20	0.90	0.60	0.40	2.50	1.50	2.00	2.10	3.40	3.1	10.5	4.60	4.90	0.50
CO_2/CH_4	5.70	172	8.80	59.50	30.30	62.70	134	152	46.30	50.80	303	172	50.3	385	101	8.50
CO_2/HCO_3^-	0.14	0.19	0.004	0.39	0.31	0.73	0.21	0.88	0.19	0.05	0.85	0.22	0.46	1.00	2.60	0.14
Cl/Br	–	285	–	23.90	26.60	–	226	1933	448	16.80	76.10	15.6	–	357	–	1.30
K/Rb	282	473	200	728	1035	375	170	368	302	512	247	383	127	456	500	466

(*continued on next page*)

Table 2 (*continued*)

Component	Darasun						Talatuy			Teremki						
	1*	2*	3*	4*	5*	6*	7*	8*	9*	10*	11*	12*	13*	14*	15*	16*
	Breccia			Veins			Ores			Veins						
Sr/Ba	0.24	4.60	69	1.30	0.60	–	1.10	2.00	1.90	13.00	0.20	4.6	3.6	3.30	8.00	1.90
Ni/Co	–	32.80	12.10	18.80	10.10	12.30	8.30	8.80	3.40	24.50	25.00	16.0	8.6	21.50	13.00	21.80
Cl/As	77	41	58	4.30	11	9.70	288	475	353	67	73	52	43	25	292	3.10
Fe/Mn	–	4.50	–	11.40	8.50	26.20	0.20	0.60	0.40	1.20	0.26	1.8	–	2.60	3.80	5.00

Notes: 1*–16*: investigations samples of quartz.

The fluid inclusion study allowed the main parameters of mineralizing fluids and evolution of fluid compositions during ore deposition at the Darasun, Talatuy, and Teremki deposits to be determined (Tables 1 and 2, Figs. 7–12).

Fluid inclusions indicate that quartz from the matrix of explosive breccia at Darasun formed at high temperature ranging from 170 to 618 °C under a pressure ranging from 170 to 1460 bars (Fig. 9). Quartz crystallized from chloride brine with a salinity ranging from 3.2% to 50.3% eq. *w*(NaCl). The fluid was immiscible (boiled) from 350 to 580 °C and tourmaline formed within this range.

Data from gas and ion chromatography indicate the following fluid composition (g/kg of solution) CO_2 10.0, CH_2 1.75, Na 27.5, K 41.8, Ca 4.4, and Mg 1.75. ICP-MS revealed the presence of a large number of trace elements with elevated concentrations of B, Rb, Mo, and Hg. The fluid shows a small CO_2/CH_4 of 5.7 indicating relatively reduced conditions.

Ore deposition at Darasun occurred at 265–445 °C and 65–2040 bar (Fig. 10). On the basis of fluid inclusions in coeval vein quartz, tourmaline crystallized at 300–445 °C and 100–2040 bar. Salinity ranges from 2.2% to 44.8% eq. *w*(NaCl). Ion chromatography indicates that the mineralizing fluid contained Na, K, and magnesium chlorides. It is concluded that tourmaline was precipitated from an immiscible fluid, and that the salinity of this fluid increased as temperature decreased, probably as a result of fluid boil-off. Below 300 °C, the trend of salinity evolution decreased with decreasing temperature suggesting introduction of meteoric water. During this event, the fluid was homogeneous, and ore deposition, including native gold, took place. Below 200 °C, the formation of a post-ore quartz–calcite assemblage completed the hydrothermal process. Data from gas and ion chromatography show the following fluid composition (g/kg of solution) CO_2 147–2.4, CH_2 4.9–0.12, Na 75–10.1, K 123–2.1, Ca 160–11.5, and Mg 31–0.9. ICP-MS data indicates elevated concentrations of As, Cu, Zn, Pb, Fe, Li, Sb, Te, and REE. For this fluid, the highest values (from all deposits) of K/Rb, Ni/Co, and Fe/Mn are 200–1035, 10.1–32.8, 4.5–26.2, respectively. The CO_2/CH_4 ratio ranges from 172 to 8.8.

Fluid inclusions indicate that ore deposition at Talatuy took place between 133 and 611 °C and 150–2310 bar. Salinity of the mineralizing fluids decreased from 55.8% to 0.4% eq. *w*(NaCl) (Fig. 11) and the immiscible (boiling) state of the mineralizing fluid corresponded to a temperature range from 611 to 310 °C. Tourmaline crystallized at 300–450 °C. Data from gas and ion chromatography indicate the following fluid composition (g/kg of solution): CO_2 50–10.5, CH_2 0.35–0.08, Na 55–47, K 27.7–20.5, Ca 18.1–11.1, and Mg 2.7–0.9. ICP-MS data reveal elevated concentrations of Sr, Ba, Mn, and Tl. In this fluid, the highest values (from all deposits) of the Cl/Br (226–1933) and Cl/As (288–475) are recorded and CO_2/CH_4 ranges from 46 to 152.

Fluid inclusions indicate that early quartz and tourmaline at Teremki were deposited from an immiscible (boiling) fluid at 300–466 °C and 80–410 bar. Salinity ranges from 1.2% to 34.7% eq. *w*(NaCl). Quartz of the productive stage was deposited from a homogeneous fluid with a salinity of 4.2%–26.4% eq. *w*(NaCl). Post-ore deposition quartz was deposited at 118–195 °C from fluid with a salinity of 2.6%–27.8% eq. *w*(NaCl). Thus, the mineralizing process at Teremki was similar to Darasun. Ore deposition began from an immiscible (boiling) fluid with decreasing temperature and pressure. Below 290 °C, the fluid became homogeneous (Fig. 12), and from gas and ion chromatography the fluid composition (g/kg of solution) was CO_2 36–6.5, CH_2 3.5–0.05, Na 29–4.5, K 15.3–0.9, Ca 73–0.5, and Mg 9.6–0.08. ICP-MS data indicates elevated

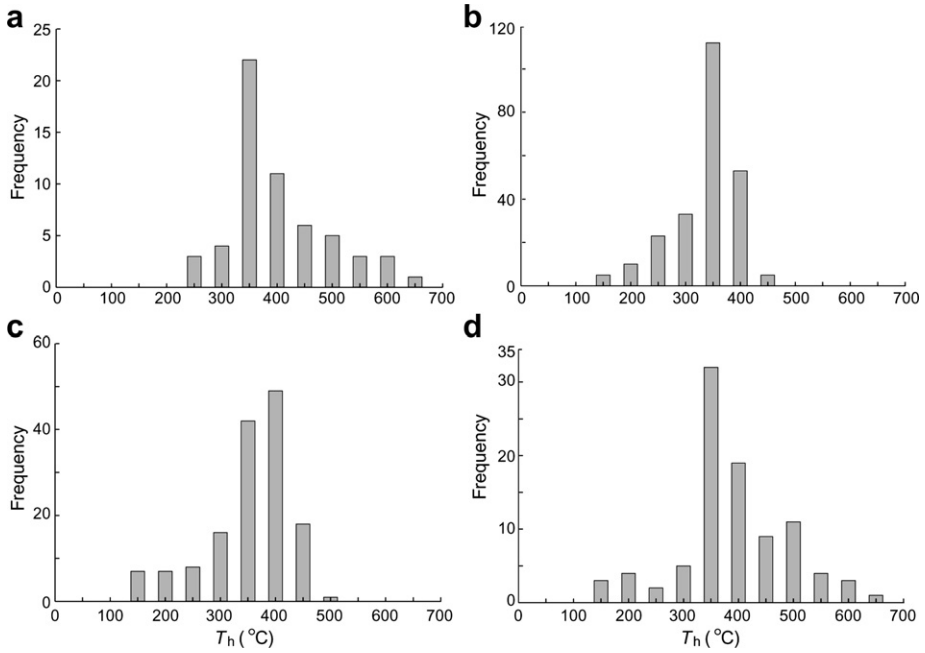

Figure 8 Histograms of total homogenizations temperatures of fluid inclusions in quartz. a: explosive breccia (disseminate ores) of Darasun deposit; b: gold ore vein of Darasun; c: gold ore vein of Teremki deposit; d: gold ores of Talatuy deposit.

concentrations of As, Cu, Zn, Pb, Fe, Li, Sb, Te, REE, with highest values (from all deposits) of K/Rb (127–512), Ni/Co (8.6–25.0) and Fe/Mn (0.26–5.0), and CO_2/CH_4 (8.5–385).

5.3. Oxygen isotope composition

Oxygen isotope composition of tourmaline from the Darasun goldfield deposits is listed in Table 3. The $\delta^{18}O$ values in studied samples range from +1.9‰ to +8.3‰.

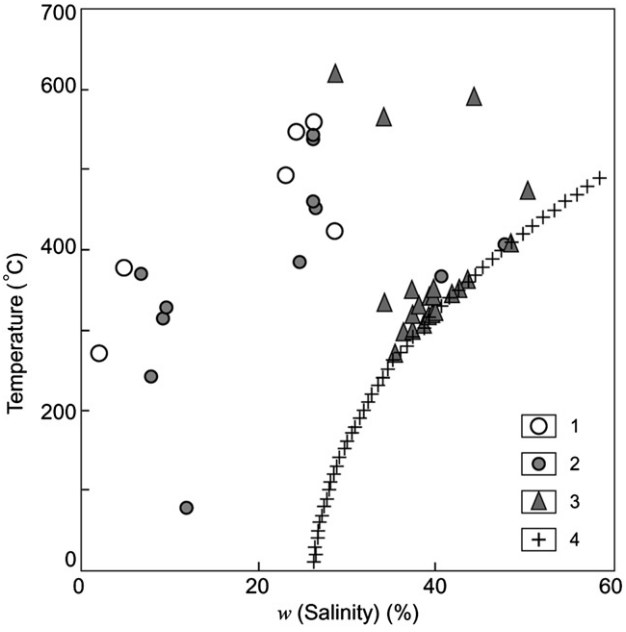

Figure 9 Plot of salinity eq. *w*(NaCl) (%) vs. temperature (°C) for fluids from quartz in the explosive hydrothermal breccia, Darasun deposit. 1: gas; 2: aqueous solution; 3: brine; 4: saturation curve of the H_2O–NaCl system.

5.4. Sm/Nd vs. Rb/Sr systematics

The Sm content in minerals from the Darasun ore veins (Prokof'ev et al., 2006) and in tourmaline from Talatuy and Teremki (new data) varies from 1.701 to 0.040 ppm; Nd ranges from 7.803 to 0.191 ppm (Table 4). There is also considerable variation in mineral Sm/Nd associated with regular variations of Nd isotope composition that allows application of the isochron model for mineralization dating. The linear trend in $^{147}Sm/^{144}Nd$–$^{143}Nd/^{144}Nd$ (6 points) (Fig. 13) indicates an isochron age of 99 ± 18 Ma (MSWD = 0.077)

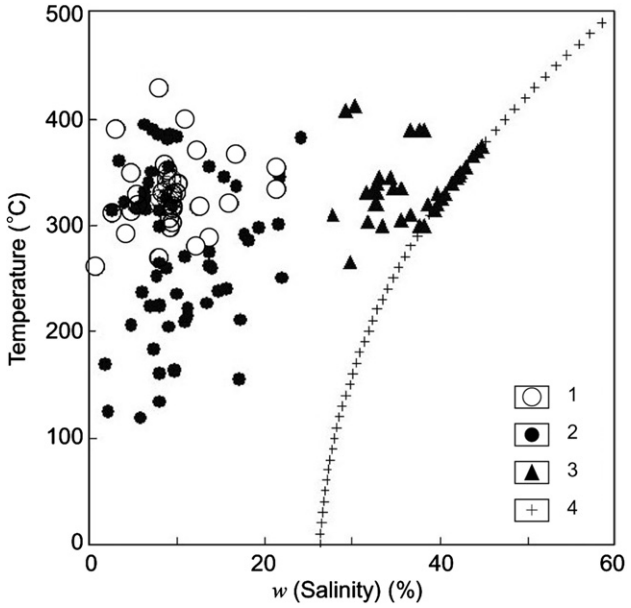

Figure 10 Plot of salinity eq. *w*(NaCl) (%) vs. temperature (°C) for mineralizing fluids in the Darasun deposit. 1: brine; 2: aqueous solution; 3: gas; 4: saturation curve of the H_2O–NaCl system.

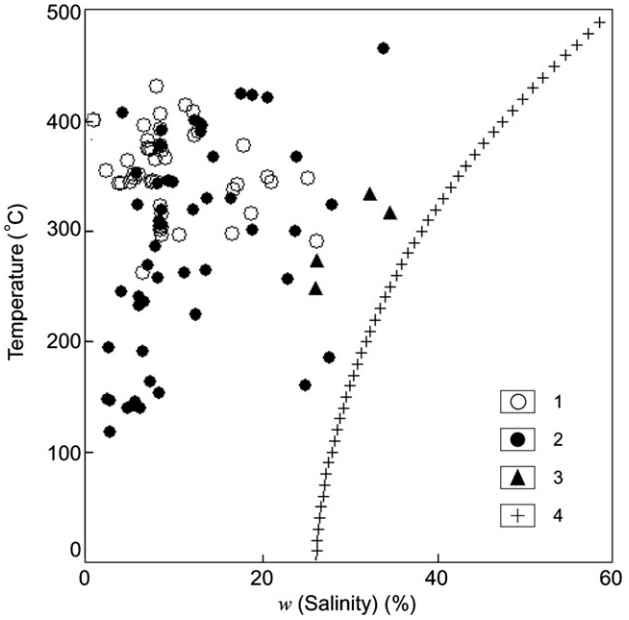

Figure 11 Plot of salinity eq. w(NaCl) (%) vs. temperature (°C) for mineralizing fluids in the Talatuy deposit. 1: brine; 2: aqueous solution; 3: gas; 4: saturation curve of the H_2O–NaCl system.

and a primary Nd isotope composition of $(^{143}Nd/^{144}Nd)_0 = 0.512478 \pm 0.000019$. Rb and Sr isotope data were not sufficient for age determination due to low Rb and a weak Rb/Sr variation in the studied minerals (Table 4). Primary isotope ratios $\varepsilon Nd(t) = -0.3 \pm 0.3$ and $(^{87}Sr/^{86}Sr)(t) = 0.7067 \pm 0.0002$ provide evidence of a crustal origin for the ore fluid source but the possibility of participation of material from chondrite-type (undepleted) mantle is not excluded (DePaolo et al., 1991).

The age of 99 ± 18 Ma for the gold ore veins at Darasun is younger than previously suggested (Prokof'ev et al., 2000). The new age is inconsistent with a collision-related genesis for the Darasun goldfield deposits and supports their relationship to Early

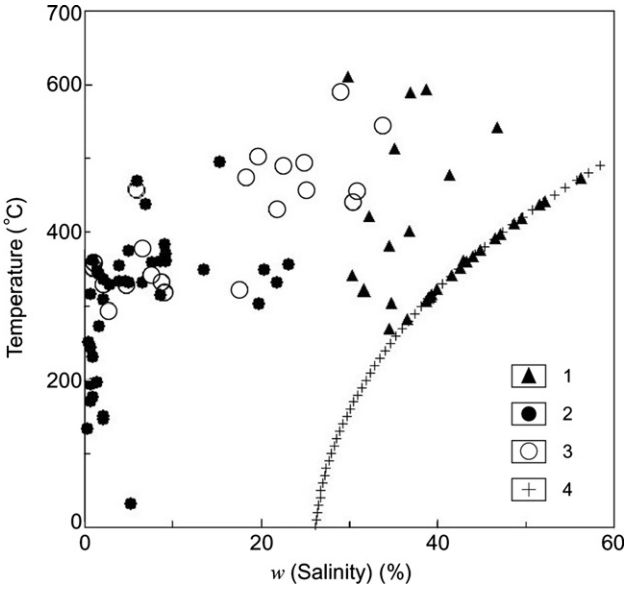

Figure 12 Plot of salinity eq. w(NaCl) (%) vs. temperature (°C) for mineralizing fluids in the Teremki deposit. 1: brine; 2: aqueous solution; 3: gas; 4: saturation curve of the H_2O–NaCl system.

Table 3 Oxygen isotope composition of tourmaline.

Sample nos.	$\delta O^{18}_{tourm\ (SMOW)}$ (‰)	T_{form} (°C)	$\delta O^{18}_{H_2O}$ (‰)
	Darasun		
1185/86	+8.3	400	+7.3
ShV3/89	+3.5	380	+2.2
260dr/85	+2.8	350	+1.0
1176dr/86	+1.9	350	+0.1
	Talatuy		
30/01	+7.6	550	+7.7
	Teremki		
878t	+6.0	350	+4.2

Notes: $\delta O^{18}_{H_2O}$ (‰) was calculated by equation of Zheng (1993): $1000 \ln\alpha = 4.210 \times 10^6/T^2 - 6.99 \times 10^3/T + 2.14$.

Cretaceous volcano-plutonic complexes associated with rifting during the development of the Mongol–Okhotsk fold belt (Zorin et al., 2001).

6. Discussion

The results of present study show that tourmaline from the Darasun goldfield crystallized under a changing geochemical environment. Dravite and Fe-rich schorl formed during the early stage characterized by oscillatory variation of fluid composition, but with an overall trend of Fe-enrichment resulting in later precipitation of Fe-richer dravite and schorl (up to povondraite- and/or buergerite-rich compositions). The increase in tourmaline Fe content is inferred to indicate decreasing temperature, relatively low $f(S_2)$ and variable $f(O_2)$. Dravite and Mg-rich schorl were precipitated during the later stage of ore deposit formation reflecting increasing $f(S_2)$ rise concomitant with early sulfide (pyrite, arsenopyrite, chalcopyrite) deposition.

Tourmalines from Darasun and Talatuy have slightly higher crystal vacancies than those from Teremki (Fig. 6), that may indicate lower pH of the mineralizing fluids in these deposits. At the same time, tourmaline from Teremki shows slightly higher Ca, which is related to their Ca-rich host rocks (gabbroids).

In ternary $Fe_{70}Al_{30}$-Al-$Mg_{70}Al_{30}$ (Fig. 6), most tourmaline compositions plot below the schorl-dravite join due to their relatively high Fe^{3+} (Slack, 1996) as indicated by Mössbauer spectra showing Fe^{3+}/Fe_{tot} ranging from 0.48 to 0.85.

Based on diagrams proposed by Fuchs et al. (2002), and taking into account the Mössbauer results and temperatures of tourmaline crystallization estimated from fluid inclusions, $f(O_2)$ values of the mineralizing fluids was ca. 10^{-25}–10^{-20}. This is much higher than that of mesothermal gold-bearing quartz veins related to the felsic intrusions and associated beresite–listwanite wall-rock alteration (Kudryavtseva and Baksheev, 2003).

The large variations of Fe^{3+}/Fe_{tot} and structural vacancies of the Darasun tourmaline suggests a wide range of $f(O_2)$ and pH of the mineralizing fluids. This is consistent with the assumption of longest duration and most complicated ore deposition of the Darasun deposit relative to other deposits of the Darasun goldfield (Prokof'ev et al., 2005a, b).

Tourmaline compositions from studied deposits show clear trend from Mg- to Fe-enrichment (Fig. 4), typical of tourmalines from the propylite zone of porphyry-copper deposits (e.g., King et al., 2000).

Table 4 Isotope composition and content (ppm) of Sm, Nd, Rb and Sr in studied minerals from gold deposits of Darasun ore field.

Sample nos.	Mineral	[Sm] ppm	[Nd] ppm	$^{147}Sm/^{144}Nd$	$^{143}Nd/^{144}Nd$	2δ	εNd	[Rb] ppm	[Sr] ppm	$^{87}Rb/^{86}Sr$	$^{87}Sr/^{86}Sr$	2δ	$(^{87}Sr/^{86}Sr)_t$
1185dr/86	Tourmaline	0.675	3.036	0.13448	0.512567	5	−0.35	2.563	1501	0.00494	0.706980	6	0.706971
1176dr/86	Tourmaline	1.068	7.803	0.08274	0.512532	10	−0.18	1.057	710.9	0.00430	0.706705	21	0.706697
170dr/85	Calcite	1.701	4.098	0.25092	0.512642	22	−0.82	1.153	220.6	0.01512	0.706636	22	0.706608
30dr/85	Arsenopyrite	0.040	0.191	0.12532	0.512560	16	−0.34	1.43	1.092	3.79139	0.713682	35	0.706677
878t/82	Tourmaline	2.027	8.882	0.13795	0.512575	5	−0.25	3.151	346.2	0.02633	0.704995	18	0.704946
30/01	Tourmaline	0.414	1.843	0.13573	0.512571	12	−0.30	14.50	484.8	0.08651	0.705789	9	0.705629

Notes: Sr and Nd isotope composition as well as Rb, Sr, Sm, Nd contents in the minerals were determined by isotope dilution method using solid phase multi-collector mass-spectrometer TRITON (CIR VSEGEI, St. Petersburg). Isotope composition for Nd standard JNdi-1 was $^{143}Nd/^{144}Nd = 0.512112 \pm 0.000003$, and Sr composition for SRM-987 was $^{87}Sr/^{86}Sr = 0.710261 \pm 0.000005$ in the course of analytical work. $\varepsilon(Nd)_T$ values were calculated supposing today CHUR parameters: $^{147}Sm/^{144}Nd = 0.1967$, $^{143}Nd/^{144}Nd = 0.512638$.

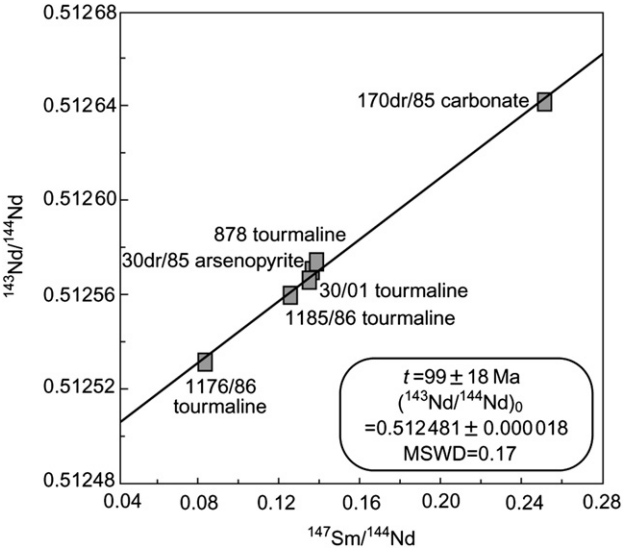

Figure 13 Sm−Nd isotope diagram for tourmaline, arsenopyrite and carbonate from ore vein of the gold deposits, Darasun gold deposits area.

High temperatures of the mineralizing fluids at the beginning of the hydrothermal process and tourmaline crystallization during the early stage of ore deposition from immiscible (boiled) fluids are typical of all the studied deposits. The mineralizing fluid pressure ranged from 65 to as much as 2310 bar, reflecting overpressures in a closed system and lower pressures when fracturing occurred, consistent with subvolcanic conditions.

Ore deposition differed at each deposit. Highest temperatures of 618 and 611 °C were detected for quartz from explosive breccia of the Darasun deposit and at the beginning of ore deposition at Talatuy, respectively. The highest pressure of (2310 bar) was documented for the Talatuy deposit. Ore deposition at Darasun and Teremki began at 430 °C and 466 °C and ranged from 120 to 430 °C and from 466 to 118 °C, respectively. Pressures during ore deposition, however, were very different, ranging from 65 to 2040 bar and from 70 to 410 bar, respectively. Unlike Darasun and Talatuy, the salinity of mineralizing fluids at Teremki did not reach chloride saturation. Highest and lowest CO_2/CH_4 values were documented in vein quartz at Teremki and in quartz from breccia at Darasun, indicating oxidizing and reducing environments, respectively. The CO_2/CH_4 ratio at Darasun goldfield deposits increased as temperature and pressure decreased (Fig. 14).

Mineralizing fluids in the studied deposits had complex chemical compositions and for each deposit shows specific geochemical

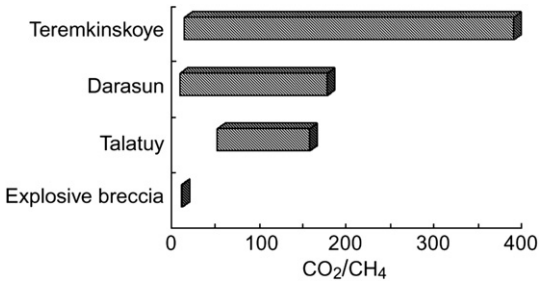

Figure 14 The CO_2/CH_4 ratio in mineralizing fluids of the Darasun goldfield deposits (Darasun, Teremkinskoye, Talatuy, and Explosive breccia of Darasun deposit).

features (Table 1). The highest concentrations of Na and K in the fluid are for quartz from explosive breccia and veins at the Darasun deposit.

Calculated $\delta^{18}O$ values for fluids responsible for tourmalinization range from +0.1‰ to +7.7‰ (Table 3). The highest values +7.3‰ and +7.7‰ are related to early high temperature tourmaline from Talatuy and Darasun, respectively, and indicate an igneous source for the mineralizing fluids (Sheppard, 1986; Kyzer and Kerrich, 1987). The lower values ranging from +0.01‰ to +4.2‰ are characteristic for lower temperature tourmalines, suggesting introduction of meteoric water into the mineralizing fluids.

Temperatures higher than 400 °C at the beginning of hydrothermal process, immiscible high salinity mineralizing fluids, and the association of K-rich igneous rocks in the studied deposits are similar to porphyry-copper deposits. A decrease of fluid salinity during the productive stage of ore formation indicates fluid dilution by low salinity meteoric water that is consistent with isotopic data.

High and variable $f(O_2)$ and mixing with meteoric water indicate a shallow level of mineralization that is consistent with an assumption of subvolcanic nature of ore-forming process at the Darasun goldfield (Prokof'ev, 2000). The above data indicate that mineralization and tourmalinization in the studied gold deposits occurred in a subvolcanic environment with variable T, p, $f(O_2)$, and pH.

An age of gold veins of 99 ± 18 Ma at Darasun implies that mineralization was related to Early Cretaceous volcano-plutonic activity associated with rifting during development of the Mongol–Okhotsk fold belt.

Acknowledgments

This work was carried out within the framework of the UNESCO-IGCP project 540 "Gold-bearing hydrothermal fluids of orogenic deposits" and the Russian Foundation for Basic Research (projects 09-05-00697 and 11-05-1207ofi-m).

Sample description of probes, Sm–Nd methods investigations.

Darasun deposit

1185dr/86 and 1176dr/86: Mine 14, level 210 m, offset Yuzhniy, veins from the Nagornaya series;

1185dr/86: vein composed of pyrite (30%), fine grained tourmaline (30%), quartz (25%–30%) and carbonate (10%) and hosted in altered granodiorite;

1176dr/86: thin vein composed of fine grained tourmaline (60%), quartz (20%), pyrite (15%), and chalcopyrite and relics of host rock (5%).

170dr/85: Mine 14, level 160 m, offset Yuzhniy, veins from the Nagornaya series. Banded vein with dark bands composed of quartz (70%), tourmaline (20%), and pyrite (10%) and light ones composed of quartz (80%) and pyrite (20%).

30dr/85: Mine 14, level 160 m, offset to vein Razvedochnaya. Veinlet composed of carbonate with impregnation of arsenopyrite, and occasional grains of sphalerite (50%), pyrite (30%) and chalcopyrite (20%). This veinlet is hosted in altered granodiorite-porphyry.

Talatuy deposit

30/01: open pit, 3rd ore zone. Tourmaline–quartz altered rock impregnated with pyrite (30%), chlorite (40%), and carbonate (30%).

Teremki deposit

878t: mine, level 155 m, place of conjunction of Ore zone 1 and vein Gornyatskaya. Quartz–tourmaline–pyrite vein hosted in altered gabbroic.

References

DePaolo, D.J., Linn, A.M., Schubert, G., 1991. The continental crustal age distribution: methods of determining mantle separation ages from Sm–Nd isotopic data and application to the Southeastern United States. Journal of Geophysical Research 96, 2071–2088.

Fuchs, Y., Lagache, M., Linares, J., 2002. Oxydation expérimentale de Fe-tourmalines et correlation avec une déprotonation des groupes hydroxyle: annealing in oxidizing conditions of Fe-tourmalines and correlated deprotonation of OH group. Comptes Rendus Geoscience 334 (4), 245–249.

King, R.W., Rabin, O.M., French, D.H., 2000. Tourmaline from Andean porphyry copper deposits. Its significance in the exploration of Andean mineralization. CSEG Conference Abstracts. www.cseg.ca/conference/2000/307.pdf.

Kudryavtseva, O.E., Baksheev, I.A., 2003. Variation in composition of tourmaline from Berezovskoye gold ore deposit, the Middle Urals. Zapiski VMO 132 (3), 108–125 (in Russian).

Kyzer, T.K., Kerrich, R., 1987. Stable isotope geochemistry of low temperature fluids. Mineralogical Association of Canada, Toronto, Ontario (Short Course) 13, 287–336.

Lyakhov, Yu.V., 1975. Temperature zonation in the Darasun deposit. Geology of Ore Deposits 2, 28–36 (in Russian).

Prokof'ev, V.Yu, 2000. Geochemical Features of Mineralizing Fluids in the Different Type Hydrothermal Gold Deposits. Nauka, Novosibirsk, 192 pp (in Russian).

Prokof'ev, V.Yu., Baksheev, I.A., Zorina, L.D., Krivitskaya, N.N., 2005a. Chemical composition of tourmaline and genesis conditions of gold mineralization in the different scale deposits of the Darasun fluid-magmatic system. In: Proceeding of International Conference "Magmatic and Metasomatic Formations and Related Mineralization", Tashkent, pp. 297–300 (in Russian).

Prokof'ev, V.Yu., Baksheev, I.A., Zorina, L.D., Krivitskaya, N.N., Ying, Zhang, 2005b. Genesis conditions of quartz–tourmaline assemblage in the different scale gold deposits (Darasun district, Eastern Transbaikalia). The Problems of Geological and Mineragenetic Correlation in the Contiguous Region of Russia, China, and Mongolia, The scientific works of the VI international symposium of geological and mineragenetic correlation in the contiguous regions of Russia, China and Mongolia and academician S.S. Smirnoff Readings. Chita, 90–94 (in Russian).

Prokof'ev, V.Yu., Baksheev, I.A., Zorina, L.D., Belyatsky, B.V., Bortnikov, N.S., 2006. The first Sm/Nd dating of gold mineralization in the Darasun deposit, Eastern Transbaikalia. Doklady Earth Sciences 49, 963–966.

Prokof'yev, V.Yu., Bortnikov, N.S., Zorina, L.D., Kulikova, Z.I., Matel, N.L., 2000. The Darasun intrusive-related gold–polimetallic deposit, Eastern Transbaikalia, Russia: petrochemical, melt and fluid inclusion, REE and stable isotope (O, C, and S) studies. In: Rammlmair, D., Mederer, J., Oberthür, Th., Heimann, R.B., Pentinghaus, H. (Eds.), Applied Mineralogy in Research, Economy, Technology, Ecology and Culture. Balkema, Rottertdam, Brookfield, pp. 399–402.

Prokof'ev, V.Yu., Bortnikov, N.S., Zorina, L.D., Kulikova, Z.I., Matel, N.L., Kolpakova, N.N., Il'ina, G.F., 2000. Genetic features of the Darasun gold–sulphide deposit (Eastern Transbaikal Region, Russia). Geology of Ore Deposits 42, 474–495.

Prokof'ev, V.Yu., Zorina, L.D., 1994. Evolution of fluids of the Darasun ore-magmatic system (Eastern Transbaikalia). Doklady Earth Sciences 335 (2), 206–209 (in Russian).

Prokof'ev, V.Yu., Zorina, L.D., 1996. Fluid regime of the Darasun ore-magmatic system (Eastern Transbaikalia) by data of fluid inclusion studies. Russian Geology and Geophysics 37 (5), 50–61 (in Russian).

Prokof'ev, V.Yu., Zorina, L.D., Baksheev, I.A., Plotinskaya, O.Yu., Kudryavtseva, O.E., Ishkov, Yu.M, 2004. Minerals and formation conditions of ores of the Teremkin gold deposit (Eastern Transbaikal region). Geology of Ore Deposits 46, 332–352.

Richard, P., Schimizu, N., Allegre, C.J., 1976. $^{143}Nd/^{144}Nd$ natural tracer: an application to oceanic basalts. Earth and Planetary Science Letters 31 (2), 269–278.

Sakharova, M.S., 1972. Stages of ore formation and zonation in the Darasun gold deposit. In: Ivensen, Yu.P. (Ed.), Ore Formation and Its Relation to Magmatism. Nauka, Moscow, pp. 213–222 (in Russian).

Sheppard, S.M.F., 1986. Characterization and isotopic variations in natural waters. Reviews in Mineralogy and Geochemistry 16 (1), 165–183.

Sillitoe, R.H., 2000. Gold-rich porphyry deposits: descriptive and genetic models and their role in exploration and discovery. Reviews in Economic Geology 13, 315–345.

Slack, J.F., 1996. Tourmaline associations with hydrothermal ore deposits. In: Grew, E.S., Anovitz, A.M. (Eds.), Boron: Mineralogy, Petrology, and Geochemistry. Reviews in Mineralogy and Geochemistry, 33(1), pp. 559–664.

Timofeyevsky, D.A., 1972. Geology and Mineralogy of the Darasun Gold Area. Nedra, Moscow, 260 pp (in Russian).

Ustinov, V.I., 1983. The procedural aspects of the light-element isotope geochemistry. In: Proceeding of All-Union Seminar Methods of Isotope Geochemistry, GEOCHI, AS USSR, p. 7 (in Russian).

Yurgenson, G.A., Yurgenson, T.N., 1995. The Darasun ore field. Deposits of Transbaikalia, Chita-Moscow. Book 2, 3–18 (in Russian).

Zheng, Y.F., 1993. Calculation of oxygen isotope fractionation in hydroxyl-bearing silicates. Earth and Planetary Science Letters 120, 247–263.

Zorin, Yu.A., Belichenko, Yu.A., Rutshtein, I.G., Zorina, L.D., Spiridonov, A.M., 1998. Geodynamics of the western Mongolian–Okhotsk fold belt and tectonic position of gold occurrences in Transbaikalia. Russian Geology and Geophysics 39, 1578–1586 (in Russian).

Zorin, Yu.A., Zorina, L.D., Spiridonov, A.M., Rutshtein, I.G., 2001. Geodynamic setting of gold deposits in Eastern and Central Trans-Baikal (Chita) Region, Russia. Ore Geology Reviews 17, 215–232.

Zorina, L.D., 1993. Formation model of gold deposits in the tectono-magmatic central type structures. Russian Geology and Geophysics 34 (2), 77–83 (in Russian).